

1 **Universal pre-mixing dry-film stickers capable of retrofitting existing microfluidics**

2 P. Delgado^{1,2}, O. Oshinowo^{1,2}, M. E. Fay^{1,2}, C. A. Luna^{1,2}, A. Dissanayaka^{1,2}, P. Dorbala^{1,2}, A. Ravindran^{1,2},

3 L. Shen^{1,2}, D. R. Myers^{1,2,3,*}

4 ¹The Wallace H. Coulter Department of Biomedical Engineering, Georgia Institute of Technology &
5 Emory University, Atlanta, GA, 30332.

6
7 ² Department of Pediatrics, Division of Pediatric Hematology/Oncology, Aflac Cancer Center and Blood
8 Disorders Service of Children's Healthcare of Atlanta, Emory University School of Medicine, Atlanta, GA
9 30322.

10
11 ³ Parker H. Petit Institute of Bioengineering and Bioscience, Georgia Institute of Technology, Atlanta, GA
12 30332.

13
14 * Corresponding Author

15 Corresponding author email: david.myers@emory.edu

16

17 Abstract

18 Integrating microfluidic mixers into lab-on-a-chip devices remains challenging yet important for
19 numerous applications including dilutions, extractions, addition of reagents or drugs, and particle
20 synthesis. High efficiency mixers utilize large or intricate geometries that are difficult to manufacture and
21 co-implement with other lab-on-a-chip processes, leading to cumbersome two-chip solutions. To that
22 end, we present a universal dry-film microfluidic mixing *sticker* that can retrofit pre-existing microfluidics
23 and maintain high mixing performance over a range of flow rates and input component mixing ratio. To
24 attach our pre-mixing sticker add-on module, one simply removes the backing material and presses the
25 microfluidic sticker onto an existing microfluidic or substrate. Our key innovation centers around the
26 multilayer use of laser-cut commercially available silicone-adhesive coated polymer sheets as microfluidic
27 layers to create geometrically complex yet easy to assemble designs that can be adhered to a variety of
28 surfaces, namely existing microfluidic devices. Our approach enabled us to assemble the well regarded
29 yet difficult to manufacture “F-mixer” in minutes, and conceptually extend this design to create a novel
30 space-saving spiral F-mixer. Computational Fluid Dynamic simulations and experimental results confirmed
31 that both designs maintained high performance for $0.1 < Re < 10$, and disparate input mixing ratios of 1:10.
32 We then tested the integration of our system by using the pre-mixer to aid in the fluorescent tagging of
33 proteins encapsulated in an existing microfluidic. When integrated with another microfluidic our pre-
34 mixing sticker successfully combined primary and secondary antibodies to fluorescently tag
35 micropatterned proteins with high spatial uniformity, unlike a traditional pre-mixing “T-mixer” sticker.
36 Given the ease of this technology, we anticipate numerous applications for point of care devices,
37 microphysiological-systems-on-a-chip, and microfluidic based biomedical research.

38
39

40 Introduction

41 When integrated into lab-on-a-chip devices, microfluidic mixers have the potential to automate
42 many laboratory steps including dilutions, extractions, addition of reagents or drugs, and particle
43 synthesis¹⁻⁷. To that end, numerous stand-alone, highly-efficient microfluidic mixers have utilized clever
44 design principles to overcome diffusion limitations that hinder microscale mixing⁸⁻¹⁰. In all cases,
45 increasing the geometric complexity of the device enhances mixing through various mechanisms
46 including: inducing transverse flows, chaotic advection¹¹, or folding flows via splitting and recombining¹².
47 Unfortunately, increased fabrication complexity typically accompanies the increased geometric
48 complexity of these devices in the form of more complex soft lithography molds or multilayer assembly
49 processes that can be difficult to co-implement with other lab on a chip processes^{13,14}.

50 Using current approaches, it remains more practical to integrate geometrically complex mixers
51 into lab-on-a-chip devices as a stand-alone component¹⁵. This multi-chip approach makes biomedical
52 research with microdevices more cumbersome and complicates translational efforts for point-of-care
53 devices. New methods, such as 3D printing^{16,17} have shown excellent potential towards improving the
54 manufacturability of integrated microfluidic devices. However, more work is needed to reduce the long
55 print times and significant process optimization for reproducible results. To complement existing
56 fabrication and 3D printing approaches, we present an easy to manufacture microfluidic pre-mixing
57 sticker that seamlessly retrofits existing microfluidics without tubing and with no change to the device
58 footprint.

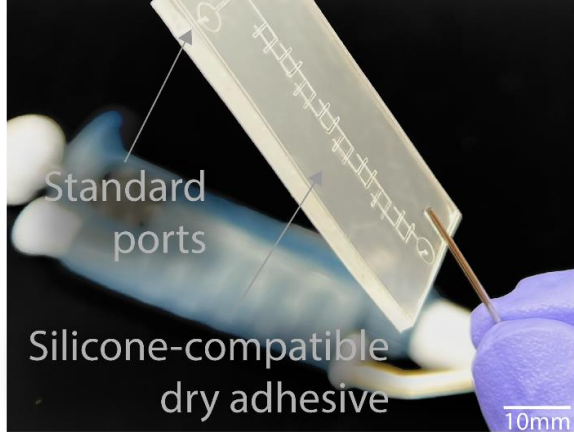
59 Our work builds on the excellent advancements of others using dry-film adhesive tape
60 technology. Dry-film adhesives have been used to micropattern and deposit materials¹⁸; create devices
61 between glass^{19,20}, wax²¹ and polymers^{22,23}; create pneumatic valves in 3D fluidics²⁴; facilitate cell
62 culture²⁵; and for use as an intermediary layer to seal channels^{26,27}. This work leverages several key

63 advantages of dry film adhesives including simple patterning with craft and laser cutters²⁸ and
64 adhesiveness to many surfaces^{29,30}. Innovative applications of using dry film adhesives for creating
65 freestanding microfluidics exist^{31,32}, including using these adhesives to simplify the mixing manufacturing
66 process³³. Building on this work, we show that silicone dry film adhesives can easily add multi-layer high
67 efficiency upstream and downstream processes to existing microfluidics.

68 Our upstream and downstream devices are essentially microfluidic “stickers” that can be peeled
69 from a backing and applied to nearly any surface with instantaneous bonding, akin to stickers used for
70 labels, signs, and amusement. Our approach, with a larger feature size set by the minimum line width of
71 the laser cutter, complements the other creative implementations of sticker-like properties for
72 microfluidics capable of smaller sized features^{34,35}. This approach also decouples the fabrication process
73 for the upstream or downstream component from the main device, and offers an alternative path to
74 monolithic integration.

75 As each layer of the dry-film adhesive readily sticks to itself and other surfaces, it greatly
76 simplifies the manufacture of geometrically complex microfluidic mixers and other structures. This
77 enables rapid fabrication of multilayer, geometrically complex, microfluidic structures while
78 circumventing the need for complex alignment processes, varying ratios of polydimethylsiloxane (PDMS)
79 polymers³⁶, integrated photoresist/PDMS processes³⁷, spun layers of PDMS³⁸, surface treatments³⁹, heat
80 mediated thermoplastic bonding⁴⁰, and more. For example, the well-regarded F-mixer¹² can be adapted
81 to a sticker format and assembled in minutes (Fig1A). Building on this simple fabrication process, we
82 now introduce a highly efficient “spiral F-mixer”, a 12-layer, small footprint device that can still be
83 assembled in minutes (Fig 1B). As mentioned, both stickers conform onto flexible surfaces (Fig 1C) or
84 retrofit existing microfluidics (Fig 1D).

A Linear F-mixing sticker



B Compact spiral F-mixing sticker

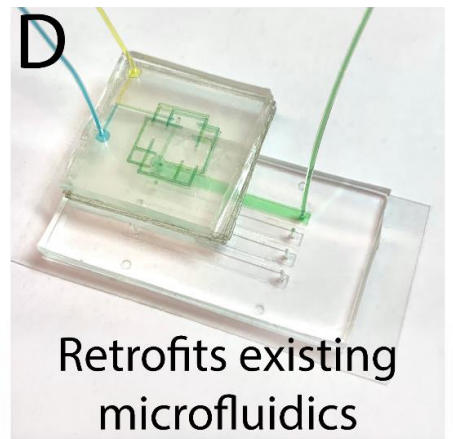
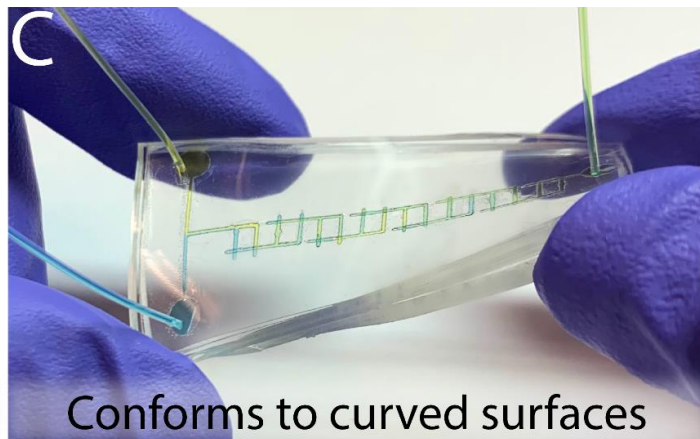
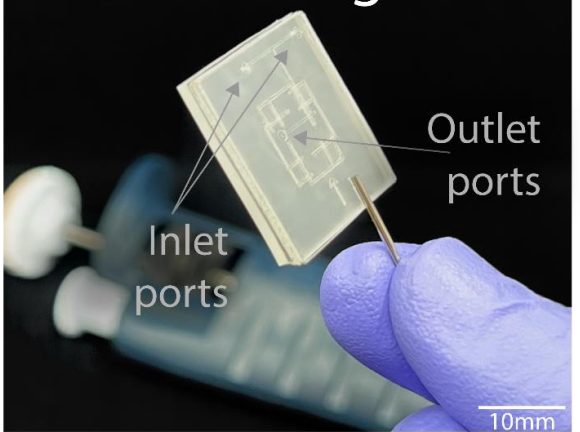


Fig 1 The versatile novel pre-mixing microfluidic stickers can be attached to any surface, including pre-existing microfluidics. A Classic Linear and **B** novel compact spiral F-mixing sticker designs shown with standard inlet and outlet ports. **C** Stickers are capable of conforming to curved surfaces when using a PDMS layer as the base. **D** Due to the silicone-compatible dry adhesive, the sticker is able to seamlessly retrofit existing microfluidics to implement an on the spot mixing step where necessary. In this configuration, the outlet port of the pre-mixing sticker aligns with the inlet port of the retrofitted microfluidic.

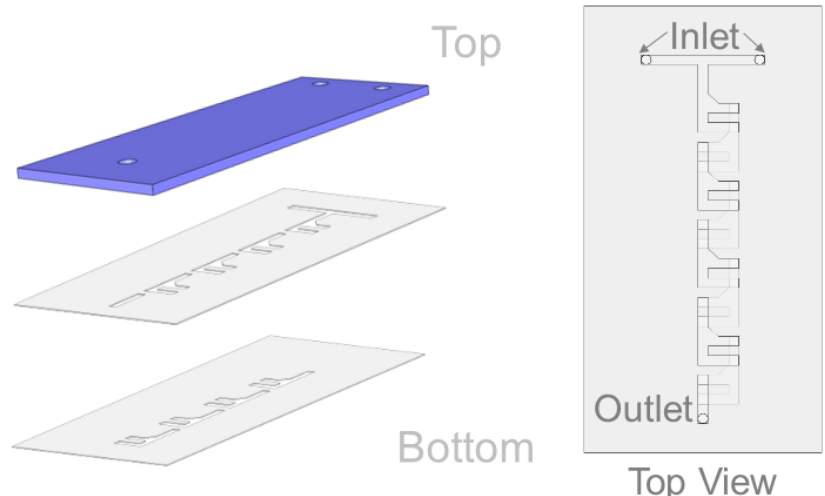
85

86 Methods and Fabrication

87 *Manufacturing Stickers*

PDMS Fluidic Interface
 3M 96042

A Linear F-Mixer



B Spiral F-Mixer

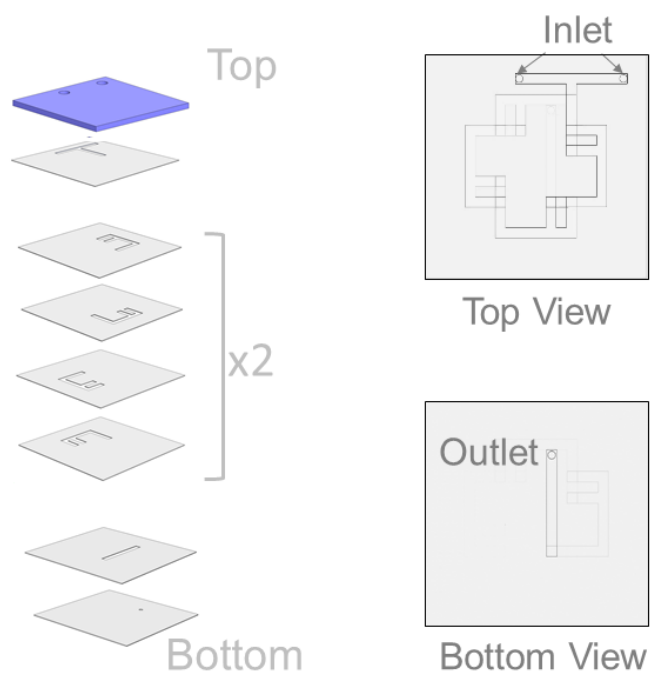


Fig 2 Laser cut dry film tape can be layered in a straightforward manner to enable geometrically complex microfluidic stickers. A The linear F-mixer comprises of 3 main layers with one PDMS fluidic interface, and two layers of 3M 96042 tape. **B** The Spiral F-Mixer is a space saving compact form of the Linear F-Mixer consisting of one PDMS fluidic interface and a total of 11 layers of 3M 96042 tape. The final bottom layer for each microfluidic is not included in the figure, but up to user preference. Shown linear F-mixer configuration is for standalone use, and the spiral F-mixer configuration can be adhered to existing microfluidic.

89 The roll-based silicone microfluidics were first drafted using Adobe illustrator. In preparation for
90 laser cutting, a non-silicone release liner (3M 5053) was layered onto the dry adhesive exposed side of
91 the 0.13mm thick roll-based silicone dry-adhesives on a polyethylene terephthalate (PET) carrier (3M
92 96042). Any air bubbles between the two layers that formed were removed by scaping the top the
93 release liner with a squeegee. The specific characteristics of silicone dry-adhesive was important in that
94 it is designed to stick to silicone surfaces unlike more commonly available double-sided tape, as acrylic
95 dry-adhesive wouldn't hold the same adhesive strength to PDMS. Selecting the silicone dry-adhesive
96 allows the sticker to have a flexible PDMS roof, and optionally have an existing PDMS microfluidic based
97 bottom layer. The combination was then used to manufacture the final pieces of tape with a laser cutter
98 (Universal Laser Systems VLS 4.60) to create the tape layers shown in Fig. 2a, b. The settings used were
99 0.13 mm for the height, and -50% quality. These settings prevented excessive scorching on the tape for
100 easier cleaning and a channel width of 200 μ m. Particulates were removed from the laser cut pieces of
101 tape via brushing off with the blunt edge of a razor blade and simple tape cleaning. A PDMS interface
102 layer was manufactured from Sylgard 184 (Dow Inc) at a standard 10:1 mixture of elastomer base:
103 curing agent. After mixing for vigorously for 1-2 minutes, the PDMS solution was degassed for 40
104 minutes and 10 grams was poured into a 100x15 mm petri dish. The PDMS interface layer was cured in a
105 65°C oven for 3-4 hours, or until use. After curing, the interface layer was peeled out of the petri dish
106 and manually cut to the dimensions of the final sticker device. The PDMS can be made in bulk
107 beforehand to save additional time when assembling the microfluidic sticker. A catheter punch (Syneo)
108 was used to create 0.75 mm \varnothing hole for the inlets and outlets. Once the sticker is complete the user can
109 select the bottom layer based off of their applications. The configurations for the linear and spiral mixer
110 shown in Fig. 2 are for the linear mixer to be used as a traditional standalone device, and the spiral
111 mixer to be retrofit. An additional configuration for the linear F-mixer to be compatible with being
112 adhered to an existing microfluidic is found in Supplemental Figure 1.

113 The stickers are built layer by layer from the top down (Fig. 3a), starting with the PDMS interface
114 layer. As shown in Fig. 3b for the linear F-mixer, a clear backing must be removed from the silicone tape
115 layer before adhering it to the PDMS fluidic interface layer. Alignment was done easily by eye, as each
116 layer was designed with tolerances to allow for minor human error during assembly. Because each piece
117 has an adhesive backing, only gentle pressure is needed to attach the first tape layer to the PDMS fluidic
118 interface layer (Fig. 3c). Before attaching the second silicone tape layer the white backing must be
119 removed from the first tape layer (Fig. 3d). The second tape layer is attached following similar steps to
120 the first one (Fig. 3e,f). When adhered to the first tape layer and PDMS layer, the linear F-mixer sticker is
121 ready to be adhered to the user's floor layer of choice (Fig. 3g). The bottom layers could consist of a
122 traditional glass slide, PDMS, a pre-existing microfluidic, or any other mixing surface of interest. The
123 spiral F-mixer is manufactured in a similar method, however requires more than two pieces of silicone
124 tape layers and a vacuum step to reduce the prevalence of bubbles blocking the channels. The F-layer of
125 the spiral fluidic has been designed to be able to be rotated 90 degrees and create as many layers as
126 necessary to mix the fluid. In this paper, eight F layers for the spiral mixer were chosen for optimal
127 mixing performance. Immediately prior to each experiment the lone spiral mixer was placed in a vacuum
128 chamber for at least an hour to eliminate bubbles prior to being adhered to a pre-existing microfluidic.
129 Within seconds of removing the tape from the vacuum chamber, the spiral mixer was attached to a floor
130 layer and 1x PBS was loaded into the channels to prime and aid in the removal of bubbles from the
131 channels. 20 μ L droplets of 1x PBS was placed at each inlet and outlet of the completed microfluidic. The
132 adhesive bond for each layer was strong, able to withstand Reynold's numbers up to ~ 23 before
133 exhibiting signs of leakage.

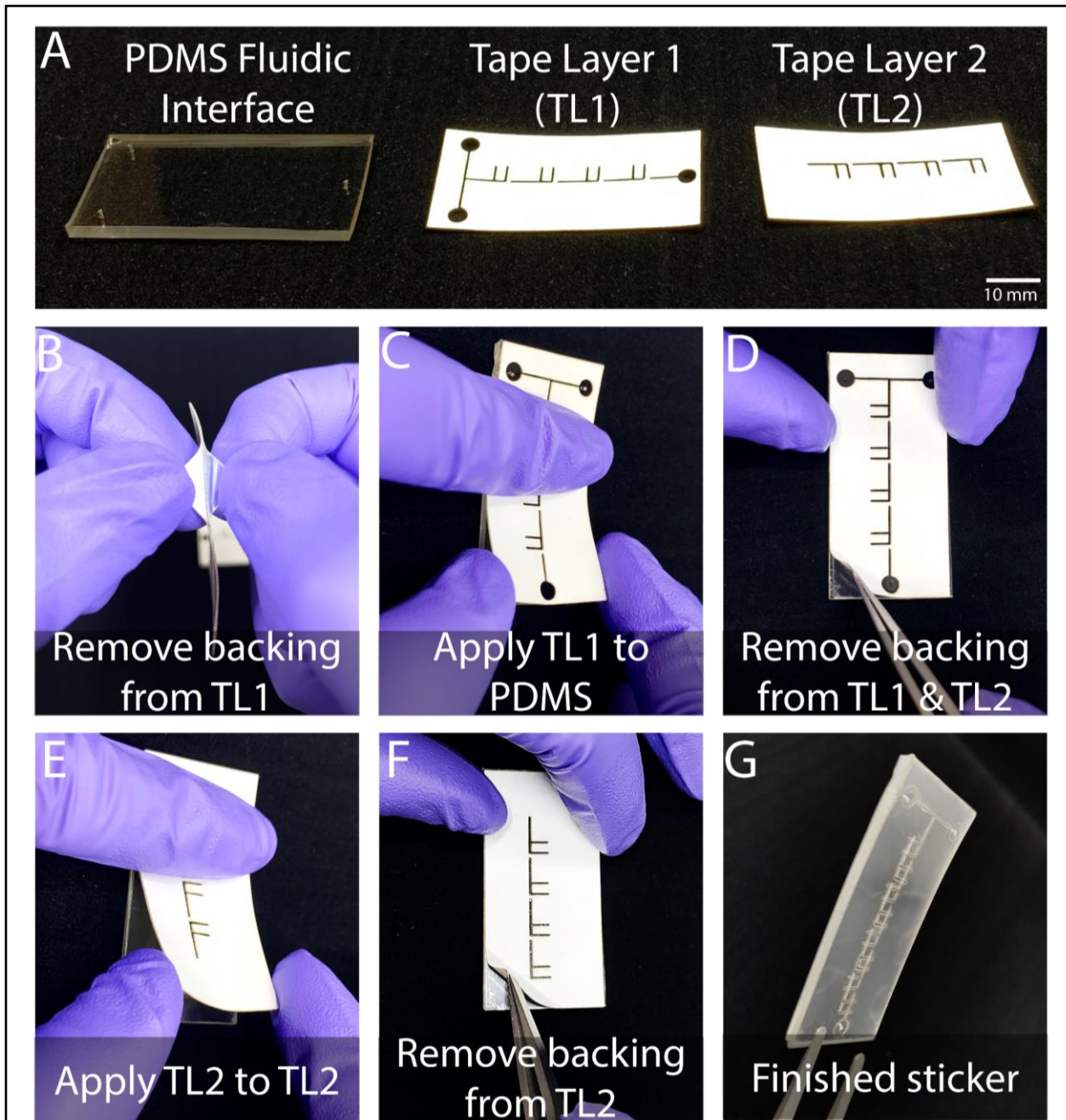


Fig 3 Sticker microfluidics can be assembled by hand in minutes. **A** Microfluidic stickers are comprised of a fluidic interface of PDMS (Sylgard 184) with multiple laser cut tape layers. **B** Each tape layer has two backing layers that must be removed during the assembly process. **C** Upon removal of the first backing layer, Tape Layer 1 can then be gently pressed onto the PDMS fluidic interface. **D** The second and final backing layer is removed from Tape Layer 1 with tweezers, and the first backing of Tape Layer 2 is removed to prepare for adhesion. **E** Tape layer 2 is applied with similar gentle pressure onto Tape Layer 2. **F** The final backing is removed from Tape Layer 2 with tweezers. **G** The finished microfluidic mixer is done and ready to be applied to the user's surface of choice.

135 *Simulated Mixing Performance*

136 Solidworks was used to create a model of the linear and spiral mixers, as shown in Figure 2. A
137 computational fluid dynamics (CFD) simulation was run in AutoCAD CFD on each model to generate
138 simulated mixing results under steady state conditions. The diffusion coefficient characteristic of
139 rhodamine 6g used for the simulations was $4 \times 10^{-10} \text{ m}^2/\text{s}^{41}$. The simulation was run at standard boundary
140 conditions of constant normal flow velocity and fixed pressures at inlets and outlet. To test the mixer's
141 ability to create an equal mixture, the mixer was tested over a range of Reynold's numbers (0.23-11.53).
142 This range was chosen to thoroughly characterize the sticker over a range that passive mixing devices
143 with simple designs, such as the T-mixer, would traditionally fail over and test the highest limits for the
144 mixer. The model was also used to simulate highly disparate mixing at the Reynold's numbers 0.1, 1, and
145 10. The disparate mixing ratios tested were from 1:0 to 1:10, increasing by increments of one.

146 *Experimental Mixing Performance*

147 Experimental data was collected from the previously mentioned mixers. The equal mixing and
148 disparate mixing were collected on a single device for the linear experiments, as well as for the spiral
149 mixer tests. The linear mixer was run by attaching it to a coverslip, and the spiral mixer was adhered to a
150 pre-existing microfluidic for the data collection. The region of interest of on the linear mixer was easy to
151 visualize. Due to the complexity of the multiple layers on pre-mixing spiral sticker, the region of interest
152 was difficult to analyze so it was placed on a separate microfluidic device. No significant changes in
153 mixing performance were expected based off of the attachment to the existing microfluidic. Multiple
154 devices were used to collect the data for the experiments. Rhodamine B (5g/L) diluted to 1:100 in pure
155 DI water was mixed with pure DI water. Two 10 mL syringes were loaded with the diluted Rhodamine
156 and DI water, one for each. The syringes were then loaded onto a syringe pump (Harvard Apparatus PhD
157 Ultra), tygon tubing (Cole-Parmer EW-06419-01) was connected via a blunt needle tip, and the lines

158 were primed prior to placing the tubing into the microfluidic. The set up was placed on the microscope
159 stage and imaged using 3D imaging with a Nikon Ti2 and CFI Plan Apochromat Lambda 20x objective (NA
160 0.75). Three 3D images were taken of the end of the channel right before the outlet over the course of 5
161 minutes. The 3D images were processed and analyzed using ImageJ. The intensities of the cross sections
162 for each 3D image were analyzed in ImageJ using the measure intensity feature and were recorded.

163 *Evaluation of Pre-Mixing Sticker Integration*

164 An array of pairs of fibrinogen microdots with a radius of 1.25 μm and separation of 4 μm were
165 patterned and stamped on plasma treated coverslips (No 1.5, 24mm \times 50mm) as described
166 previously^{42,43}. Briefly, the microdot pattern was created by a silicon mold using standard lithography
167 and etching techniques. Fibrinogen (Enzyme Research Laboratory) was incubated on square (10 mm x 10
168 mm x 3 mm) polydimethylsiloxane (PDMS) at 30 $\mu\text{g}/\text{mL}$ for 30 minutes at 37 degrees before being rinsed
169 with water and dried with nitrogen gas. These fibrinogen coated PDMS squares were then placed onto
170 the plasma treated silicon mold in order to create the microdot patterned PDMS “stamp”. Two
171 micropatterned “stamps” were then placed side by side on to a plasma treated 24 mm x 50 mm
172 coverslip and subsequently blocked with 1% BSA before experimentation. A simple four channel
173 microfluidic was laser cut from the roll-based silicone to create the channels for the microfluidic and
174 adhered to the coverslip containing the “stamp”. A PDMS roof containing inlets and outlets was then
175 placed on top of the four channel tape channels, and 1% BSA was pipetted into the channels.

176 To explore a functional application for the mixer, we assessed its ability to work for binding
177 primary and secondary antibodies to fluorescently tag microdots. The spiral F-mixer was utilized to be
178 retrofit to a pre-existing microfluidic that contained the micropatterned dots. Equal amounts of two
179 different antibodies were flowed into the channels at a Reynold’s number of 0.23. The primary antibody,
180 mouse Anti-Human fibrinogen monoclonal antibody (Enzyme Research Laboratory), was mixed with 1%

181 BSA solution (1:40). The secondary antibody, Alexa Fluor 488 tagged Goat Anti- Mouse antibody
182 (Thermofisher), was mixed with 1% BSA solution (1:80). Total Internal Reflectance Fluorescence (TIRF)
183 microscopy was used to capture fluorescent images of the antibodies binding to the micropatterned
184 dots over 20 minutes. The resulting images were then analyzed via custom Python script to capture and
185 record the increasing intensity of the dots over time using region property analysis implemented with
186 scikit-image⁴⁴.

187 To further compare the F-mixer's efficiency against a traditional T mixer, a T mixer was laser cut
188 from the same roll-based silicone used to make the F-mixers and adhered to a pre-existing microfluidic
189 similar to that of the spiral F-mixer. The T-mixer was cut to have a similar footprint as the spiral F-mixer.
190 An additional T-mixer was laser cut that shared the approximate total length (70mm) of the spiral F-
191 mixer was also created for supplemental data. The primary antibody, sheep Anti-Human fibrinogen
192 monoclonal antibody (Enzyme Research Laboratory), was mixed with 1% BSA solution (1:40). The
193 secondary antibody, Alexa Fluor 488 tagged Donkey Anti- sheep antibody (Thermofisher), was mixed
194 with 1% BSA solution (1:80). A sheep antibody was used to assess mixing performance across different
195 sources. The primary and secondary antibodies were flowed through the channels of the T and F mixer
196 at a flowrate of 10 $\mu\text{L}/\text{min}$. After 5 minutes, the flow was stopped and the channels were flushed with
197 200 μL of 1x PBS three times. Fluorescent images of the antibodies binding to the microdots were then
198 taken over the entire surface to quantify the spatial uniformity.

199

200 Results

201 *Linear and Spiral F-Mixer Design*

202 The linear F-mixer design follows the traditional injection molded F-mixer design, consisting of
203 two inlets and one outlet. As each fluid goes in through their respective inlet, the two fluids meet at the

204 beginning of a T mixer before being split through the first F in the series. While going through the series,
205 the fluids will be continuously split and then recombined to ensure that mixing is not reliant only on
206 diffusion like a “T-mixer”. The spiral F-mixer represents a conceptual extension of the classic F-mixer
207 that leverages our rapid manufacturing process. Each split and recombine process also features a 90-
208 degree rotation. The layers for each F were designed to be interchangeable, one simply rotates each
209 subsequent layer by 90 degrees to connect to the previous layer. This particular aspect helps simplify
210 the design and assembly by having only 4 unique device layers. This 90-degree rotation after each split
211 and recombine allowed for a significant reduction in the area of the device. From a design perspective,
212 the spiral F-mixer utilizes approximately 50% less space than the linear F-mixer. Both sticker microfluidic
213 modules are easily implemented onto virtually any surface and can be assembled in minutes. In
214 addition, our multilayer design approach can be conceptually extended further to include more layers.

215

216

217

218

219

220

221

222

223

224

225

226 *Simulations*

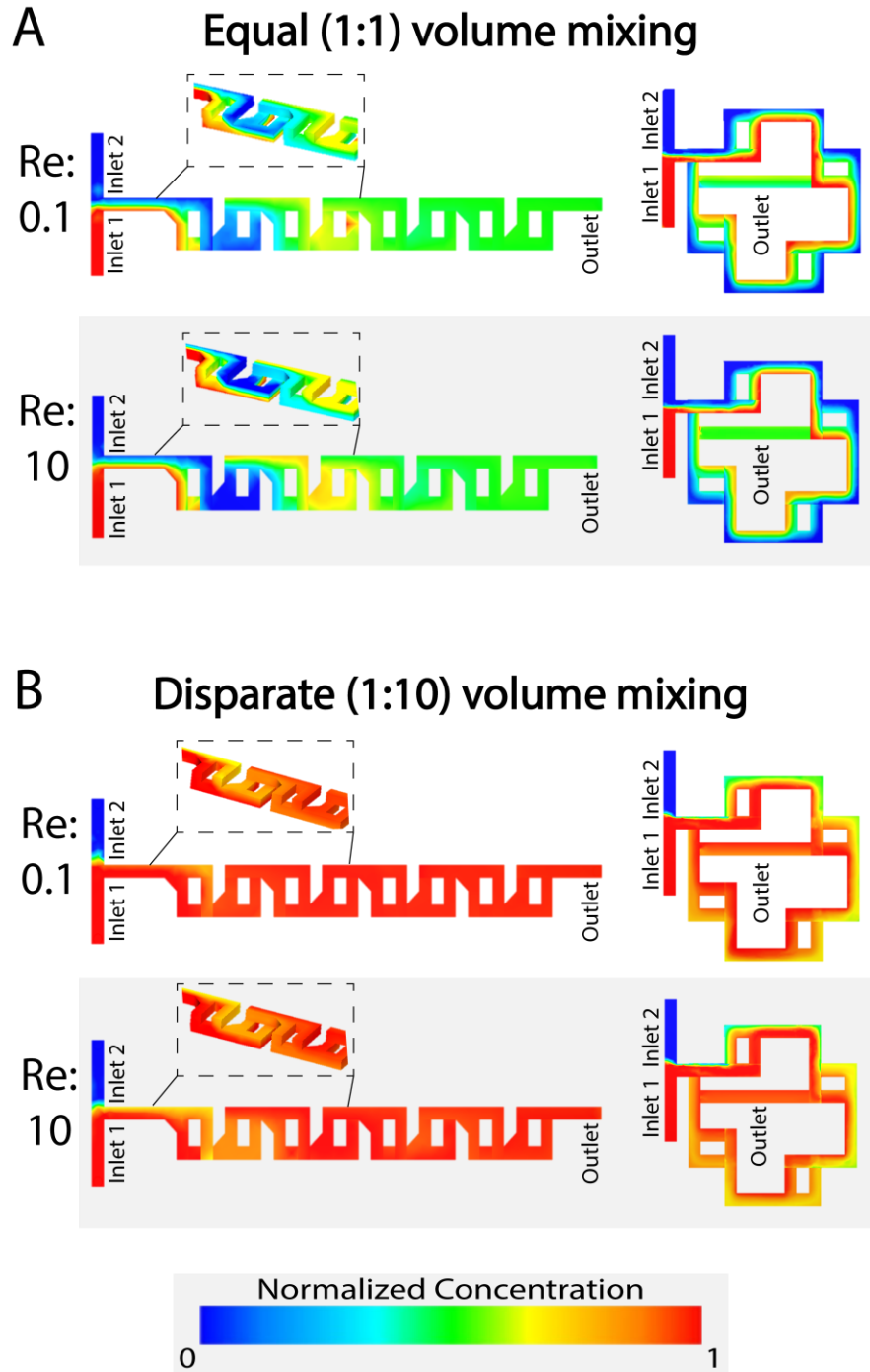


Fig 4 Our simulations predict that both mixers will have high mixing performance for different flow rates and input volume ratios. **A** The linear and spiral F-mixing stickers are able to mix a 1:1 ratio of equal volume mixing over low (0.1) and high (10) Reynold's numbers consistently. **B** The pre-mixing stickers are also capable of thoroughly mixing highly disparate volumes at a 1:10 ratio low (0.1) and high (10) Reynold's numbers.

228 The simulations run on AutoCAD CFD showed that the linear and spiral mixer were able to mix
229 reliably over a range of Reynold's numbers as shown in Fig. 4. Excellent mixing performance was
230 predicted for high (10) and low (0.1) Reynold's numbers as well as for varying volumetric ratios of
231 inputs, from 1:1 to 1:10. Beginning first with mixing equal ratios of each fluid, at a low Reynold's number
232 (Re= 0.1) the final concentrations were 0.502 and 0.514 for the linear and spiral mixers, respectively (Fig.
233 4a). When simulated at a high Reynold's number (Re= 10) the values were 0.505 and 0.517 (Fig. 4a).
234 Both cases are close to the ideal 0.5 expected for perfect mixing. The mixer exhibited a comparable
235 performance when mixing highly disparate volumes. When mixed at a 1:10 ratio at a low Reynold's
236 number of 0.1 the linear mixer's concentration was 0.945 and spiral mixer's concentration was 0.929
237 (Fig. 4b). The high Reynold's number of 10 the linear and spiral mixers concentrations were 0.959 and
238 0.929, respectively (Fig. 4b). Again, this was close to the theoretical 0.909 that would be expected for
239 perfect mixing.

240

241

242

243

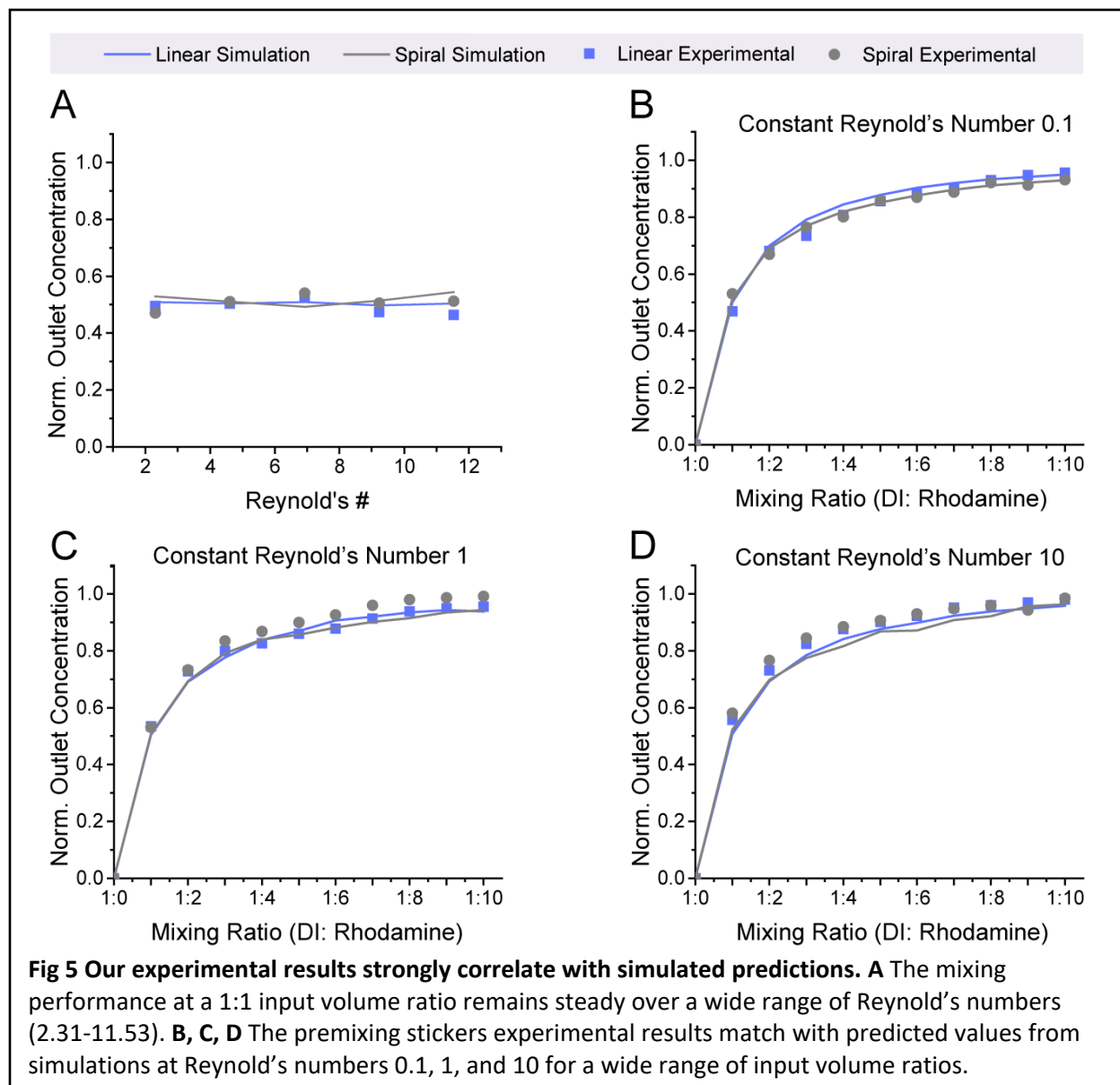
244

245

246

247

248



250

251 Our experimental results show that the mixers have excellent performance that closely aligns
 252 with the predicted simulated results for a range of flowrates and disparate mixing ratios. To thoroughly
 253 characterize the mixing for the microfluidic, the mixer's performance was first evaluated over a range of
 254 Reynold's numbers from 2.31-11.53, which is a range that encompasses flow rates that would not be
 255 conducive to mixing with a traditional passive mixer. A Reynold's number of 0.02 would be needed for

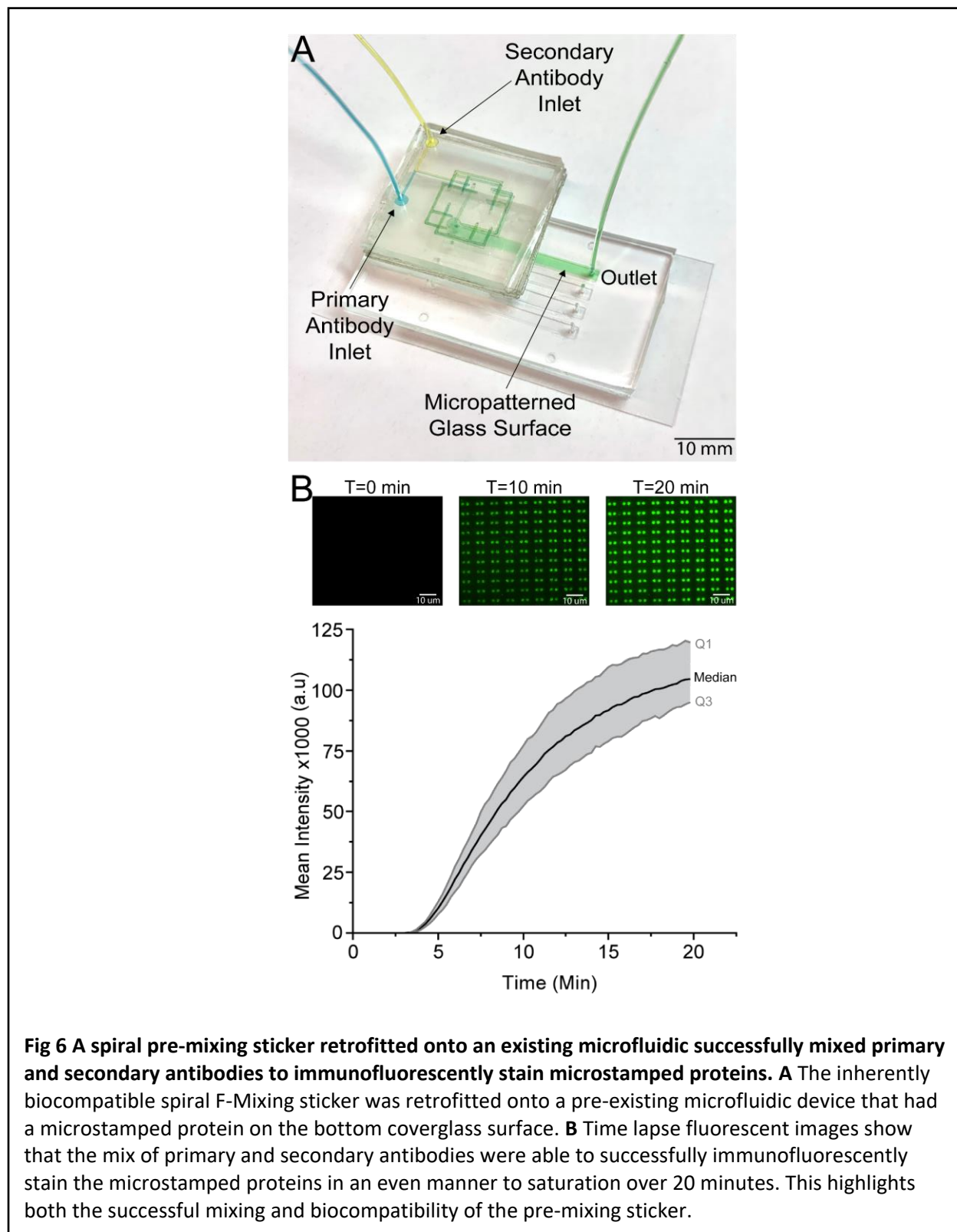
256 successful mixing with a comparatively sized (similar channel width) diffusion-based T-mixing sticker.
257 Our results showed that the linear and spiral simulations strongly correlated with the experimental
258 values, as shown in Fig. 5a for both the linear and spiral F-mixers. To continue to test the performance of
259 the F-mixers, disparate mixing was performed via simulation and experimentally. The mixing was tested
260 at three different conditions (Re # 0.1, 1, 10). At Reynold's number 0.1, the values very closely
261 correlated with the simulated values (Fig. 5b). As the Reynold's number increased, the mixed
262 concentration values continued to follow the trend that was set by the simulated results with very minor
263 deviations (Fig. 5c, d). Additional simulations were run to assess whether or not the addition of adhering
264 the sticker to an existing device would alter the mixing of the mixers. This was shown to have no
265 significant change in the mixing efficiency (Supplemental Fig. 2).

266 *Manufacturing Optimization*

267 We found that careful and consistent pressure during assembly was key to consistent high
268 mixing performance. The best results were achieved by a light tapping pressure applied throughout the
269 surface of each tape layer during manufacturing. When the assembly pressure is too high, channel
270 collapse and/or collapse of the port structures could obstruct the channels and reduce the mixing
271 efficiency. Optimization of the laser cutting parameters to reduce burning on the edges of the tape was
272 also essential to maintain proper mixing. Excessive burning on the edges of the channels resulted in
273 particulates that were hard to reduce during the sticker layer procedures which would in turn release
274 particulates into the downstream microfluidic and pre-mixing sticker. Throughout testing, the spiral
275 mixer showed a non-symmetric nature, seemingly favoring one side over the other rather than showing
276 no preference like the linear mixer, at a 10:1 ratio with splitting and mixing the streams of fluids. This
277 resulted in minor streamlines of high and low concentration through the channel. This was found to
278 have negligible deviations in the mixing performance, as it could be eliminated by switching the inlets

279 that each solution would flow through. The inlet with the highest amount of volume flowing through it
280 tended to work best when being at inlet 1, shown in Fig 4.

281



284 Mixing primary and secondary antibodies immediately prior to labeling a microstamped protein
285 exemplifies the key strengths of our sticker-based microfluidics. The tape used for the sticker has been
286 shown previously to be
287 did not disturb or alter micropatterned proteins, as shown with the initial sticker microfluidic that was
288 adhered to the surface to create simple straight channels followed by a pre-mixing sticker (Fig. 6a). The
289 unlabeled primary antibody mixed with the labelled secondary antibody and the successful product of
290 the mixture was shown on the microdots. As time passed and more of the antibodies continued to mix
291 and flow through the channels the intensity of the microdots continued to increase (Fig. 6b). The
292 microdot intensity continued to increase until the microdots were saturated with bound antibodies. The
293 spiral F-mixer sticker was shown to easily be able to mix two antibodies and distribute the completely
294 mixed antibodies throughout the channel.

295

296

297

298

299

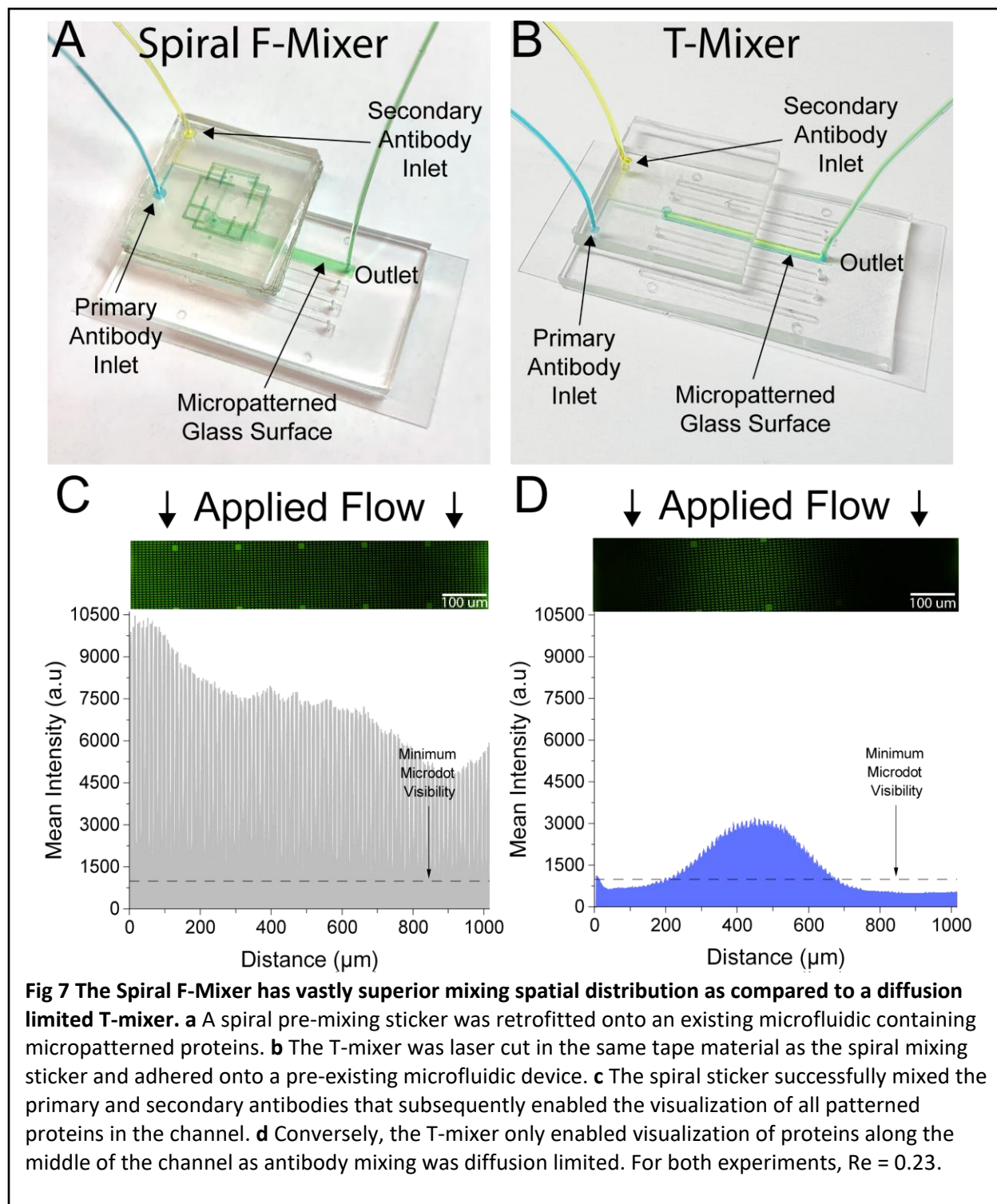
300

301

302

303

304



307 In addition to showing the mixer's biocompatibility and ability to pre-mix two components, we
308 also wanted to test the spatial performance of the mixer, and how well distributed these components
309 were. For a control, we created a standard T-mixer with a similar footprint to our F-mixer, in which two
310 streams meet and mixing is performed exclusively via diffusion. Both our spiral F-mixer and a traditional
311 T-mixer were adhered upstream of a straight channel microfluidic, with a width of ~ 0.2 mm (Fig. 7a,b).
312 The results in Fig. 7c,d showed that at the same Reynold's number ($Re = 0.23$) as the spiral F-mixer, the
313 T-mixer performance was suboptimal. This was clearly shown with the bright line in the middle of the
314 channel showing a successful mix of the antibodies surrounded by significantly less bright microdots
315 (Fig. 7d). Dark areas on the T-mixer indicate the absence of either the primary or secondary antibody
316 since both are needed to generate a fluorescent signal. In comparison, the spiral F-mixer outperformed
317 the T-mixer and had a well distributed brightness of the microdots enabling the visualization of every
318 protein microdot across the channel (Fig. 7c). The T-mixer, also, showed about half of the fluorescent
319 intensity when compared to the spiral F-mixer, potentially indicating that there was less successful
320 mixing done overall. A long T-mixer with similar total channel length to the spiral F-mixer was created in
321 order to investigate the contribution of geometry to mixing. Similar to the shorter T-mixer, it was found
322 to have half of the overall fluorescent intensity as the spiral F-mixer (Supplemental Fig 3). Important to
323 note, while collecting the longer T-mixer system proved to be suboptimal and cumbersome for practical
324 applications as the existing microfluidic and long T-mixer combination didn't fit on to a traditional
325 microscope stage meant for microscope slides. As a result, the mixer had to be carefully cut with a blade
326 to be able to load the existing microfluidic onto the microscope stage and collect the data. Additionally,
327 insufficient mixing can be seen clearly by eye when comparing the long T-mixer with the F-mixer at
328 various Reynold's numbers (Supplemental Fig 4).

329 Discussion

330 In this paper, we demonstrate a novel universal mixing sticker. The key innovation was
331 implementing the laser-cut silicone-adhesive coated polymer sheet to create the once complex to
332 manufacture F-mixer. The sticker was utilized to not only easily create multilayer designs, but also
333 revamped this design by creating the first to our knowledge spiral F-mixer. The spiral F-mixer not only
334 decreases the amount of surface area required for the mixer, but also showcases the polymer's ability to
335 build multilayer structures with ease. This paper aptly characterizes a linear (traditional) F-mixing sticker
336 and the spiral F-mixing sticker to compare it against the F-mixers previously published performance.
337 Upon characterization, the mixer is applied to mix primary and secondary antibodies on a
338 micropatterned microdot array to exemplify its ability to distribute an even mix throughout the channel.
339 As a final testament to its superior design, the same experiment was conducted and compared against
340 the performance of a T-mixer. The results demonstrated promising performance of the stickers being
341 able to mix not only at a range of Reynold's number, but also disparate volumes lending this technology
342 to limitless applications.

343 For decades classic microfluidic mixers have traditionally been difficult to manufacture and
344 integrate into microfluidic devices. To our knowledge, this paper was the first introduction to a new
345 paradigm of universal sticker microfluidic mixers that are simple to manufacture, flexible, and adapt to
346 any application via their ability to retrofit pre-existing microfluidics and work reliably over a wide range
347 of Reynold's numbers. The revamped F-mixers mirrored the CFD simulation, and were able to mix highly
348 disparate volumes despite being tested over three different magnitudes of Reynold's numbers. Mixing
349 primary and secondary antibodies showcased this technology's limitless potential for different
350 applications, as well as confirming its ability to outperform a T-mixer. The mixer's strong performance
351 opens the doors for sticker microfluidics to change the way we think about microfluidics as a whole.

352 Our dry-film sticker microfluidics could find broad use in basic biomedical research utilizing
353 microfluidics. While several implementations of double coated adhesive tape layers have been used as

354 interfaces for sensors, surprisingly few implementations have been done on biologically active surfaces.
355 For example, our approach to can create simple microfluidic channels that attach to biologically active
356 micropatterned surfaces that are often used in hematology research ⁴⁵⁻⁴⁷. Moreover, our pre-mixer can
357 be added to existing devices to enable integrated on-chip re-coagulation of whole blood by mixing
358 whole blood with CaCl₂, especially as our mixer is agnostic to the flow speed or mixing ratio. Such an
359 approach would replace existing 2 chip approaches ^{15,48}, and solve the issue of recalcified blood clotting
360 in upstream syringes/tubes. As our bonding process is non-destructive, it can also simplify point-of-care
361 assay assembly by enabling sticker microfluidics to be added on top of microspotting & lyophilization of
362 key reagents on simple flat substrates ^{49,50}.

363 More broadly, the ability to add up- and down-stream processes to existing microfluidics could
364 prove useful in a variety of settings. As many point-of-care devices require some sample preparation
365 before use, upstream processes to dilute samples or extract biomarkers may help such devices begin to
366 bridge the translational gap by making them easier to use. Our dry film sticker technology could also be
367 adapted to add inexpensive commercially available upstream filters to existing point-of-care devices, to
368 enable them to process more complex patient samples such as blood, urine, sweat, and saliva.
369 Traditional approaches of sample processing in microfluidics consist of separate systems that are either
370 designed in with the rest of the point-of-care devices or a separate entity of its own that gets connected
371 via tubing⁵¹. The seamless integration to existing microfluidics and reduction of the overall surface area
372 frames the sticker microfluidic as an attractive option to continue to innovate better point-of-care
373 microfluidics.

374 For microphysiological systems on a chip, our dry film sticker approach could open up the option
375 of integrating upstream bubble traps to help protect long term cell cultures from catastrophic damage
376 due to bubbles. Many bubble traps have been designed to be incorporated within the microfluidic⁵².
377 This would save from having to redesign the microfluidic to include a bubble trap, in the case that the

378 case of air bubbles wasn't identified until after the microfluidic platform was tested. The modularly
379 added bubble trap to the existing microfluidic platform could then be loaded with cells. The weeks and
380 months saved from having another mold made in the cleanroom to address this would significantly
381 reduce the overall amount of time spent troubleshooting.

382 Sticker microfluidics offer many remarkable advantages to traditional microfluidics. The
383 seamless incorporation into existing microfluidics, sticker or traditional, allows for endless modular
384 customization of microfluidics. The sticker will find many uses not only in integration, but also when
385 used with surfaces that need to be preserved without the need for tedious manufacturing steps. The
386 benefits are infinite in sample preparation, mixing and manipulation of fluids regardless of the
387 application at hand.

388

389 Conflict of Interests

390 The authors declare no competing interests.

391

392 Author Contributions

393 P. Delgado designed CAD for the microfluidics, ran simulations on the CAD, fabricated microfluidic
394 devices, ran experiments, and drafted manuscript. O.O. assisted with running antibody experiments,
395 analyzing data, creating figures, and helped draft manuscript. M.E.F. developed the Matlab code and
396 analyzed antibody experiments. C.A.L. assisted with the fabrication of microfluidic devices and running
397 experiments. A.D. assisted with fabrication and preparation of microfluidic devices as well as running
398 experiments. P. Dorbala assisted with the design of the microfluidics and characterization of
399 microfluidics. A.R. assisted with the design of the microfluidics and characterization of microfluidics. L.S.

400 assisted with antibody experiments. D.R.M. oversaw microfluidic design and analysis, and revised the
401 manuscript.

402

403 References

- 404 1. Dineva, M. A., MahiLum-Tapay, L. & Lee, H. Sample preparation: a challenge in the development of
405 point-of-care nucleic acid-based assays for resource-limited settings. *Analyst* **132**, 1193–1199
406 (2007).
- 407 2. Waggoner, J. J. & Pinsky, B. A. Comparison of automated nucleic acid extraction methods for the
408 detection of cytomegalovirus DNA in fluids and tissues. *PeerJ* **2**, e334 (2014).
- 409 3. Kuan, D.-H., Wu, C.-C., Su, W.-Y. & Huang, N.-T. A Microfluidic Device for Simultaneous Extraction of
410 Plasma, Red Blood Cells, and On-Chip White Blood Cell Trapping. *Sci. Rep.* **8**, 15345 (2018).
- 411 4. Imran, J. H. & Kim, J. K. A Nut-and-Bolt Microfluidic Mixing System for the Rapid Labeling of
412 Immune Cells with Antibodies. *Micromachines (Basel)* **11**, (2020).
- 413 5. Lim, J.-M. *et al.* Ultra-high throughput synthesis of nanoparticles with homogeneous size
414 distribution using a coaxial turbulent jet mixer. *ACS Nano* **8**, 6056–6065 (2014).
- 415 6. Mukherjee, A. *et al.* Lipid-polymer hybrid nanoparticles as a next-generation drug delivery
416 platform: state of the art, emerging technologies, and perspectives. *Int. J. Nanomedicine* **14**, 1937–
417 1952 (2019).
- 418 7. Zhigaltsev, I. V. *et al.* Bottom-up design and synthesis of limit size lipid nanoparticle systems with
419 aqueous and triglyceride cores using millisecond microfluidic mixing. *Langmuir* **28**, 3633–3640
420 (2012).
- 421 8. Mengeaud, V., Josserand, J. & Girault, H. H. Mixing processes in a zigzag microchannel: finite
422 element simulations and optical study. *Anal. Chem.* **74**, 4279–4286 (2002).

- 423 9. Raza, W., Ma, S.-B. & Kim, K.-Y. Multi-Objective Optimizations of a Serpentine Micromixer with
424 Crossing Channels at Low and High Reynolds Numbers. *Micromachines (Basel)* **9**, (2018).
- 425 10. Salieb-Beugelaar, G. B., Gonçalves, D., Wolf, M. P. & Hunziker, P. Microfluidic 3D Helix Mixers.
426 *Micromachines (Basel)* **7**, (2016).
- 427 11. Liu, R. H. *et al.* Passive mixing in a three-dimensional serpentine microchannel. *J. Microelectromech.*
428 *Syst.* **9**, 190–197 (2000).
- 429 12. Kim, D. S., Lee, S. H., Kwon, T. H. & Ahn, C. H. A serpentine laminating micromixer combining
430 splitting/recombination and advection. *Lab Chip* **5**, 739–747 (2005).
- 431 13. Scott, S. M. & Ali, Z. Fabrication Methods for Microfluidic Devices: An Overview. *Micromachines*
432 *(Basel)* **12**, (2021).
- 433 14. Niculescu, A.-G., Chircov, C., Bîrcă, A. C. & Grumezescu, A. M. Fabrication and Applications of
434 Microfluidic Devices: A Review. *Int. J. Mol. Sci.* **22**, (2021).
- 435 15. Lehmann, M. *et al.* On-chip recalcification of citrated whole blood using a microfluidic herringbone
436 mixer. *Biomicrofluidics* **9**, 064106 (2015).
- 437 16. Kuo, A. P. *et al.* High-Precision Stereolithography of Biomicrofluidic Devices. *Adv Mater Technol* **4**,
438 (2019).
- 439 17. He, Y., Wu, Y., Fu, J.-Z., Gao, Q. & Qiu, J.-J. Developments of 3D Printing Microfluidics and
440 Applications in Chemistry and Biology: a Review. *Electroanalysis* **28**, 1658–1678 (2016).
- 441 18. Levaché, B., Azioune, A., Bourrel, M., Studer, V. & Bartolo, D. Engineering the surface properties of
442 microfluidic stickers. *Lab Chip* **12**, 3028–3031 (2012).
- 443 19. Greer, J., Sundberg, S. O., Wittwer, C. T. & Gale, B. K. Comparison of glass etching to xurography
444 prototyping of microfluidic channels for DNA melting analysis. *J. Micromech. Microeng.* **17**, 2407
445 (2007).
- 446 20. Neuville, A. *et al.* Xurography for microfluidics on a reactive solid. *Lab Chip* **17**, 293–303 (2017).

- 447 21. Jeong, S.-G., Lee, S.-H., Choi, C.-H., Kim, J. & Lee, C.-S. Toward instrument-free digital
448 measurements: a three-dimensional microfluidic device fabricated in a single sheet of paper by
449 double-sided printing and lamination. *Lab Chip* **15**, 1188–1194 (2015).
- 450 22. Martínez-López, J. I., Mojica, M., Rodríguez, C. A. & Siller, H. R. Xurography as a Rapid Fabrication
451 Alternative for Point-of-Care Devices: Assessment of Passive Micromixers. *Sensors* **16**, (2016).
- 452 23. Gerber, L. C., Kim, H. & Riedel-Kruse, I. H. Microfluidic assembly kit based on laser-cut building
453 blocks for education and fast prototyping. *Biomicrofluidics* **9**, 064105 (2015).
- 454 24. Cooksey, G. A. & Atencia, J. Pneumatic valves in folded 2D and 3D fluidic devices made from plastic
455 films and tapes. *Lab Chip* **14**, 1665–1668 (2014).
- 456 25. Stallcop, L. E. *et al.* Razor-printed sticker microdevices for cell-based applications. *Lab Chip* **18**, 451–
457 462 (2018).
- 458 26. Bartolo, D., Degré, G., Nghe, P. & Studer, V. Microfluidic stickers. *Lab Chip* **8**, 274–279 (2008).
- 459 27. Neckel, I. T. *et al.* Development of a sticker sealed microfluidic device for in situ analytical
460 measurements using synchrotron radiation. *Sci. Rep.* **11**, 23671 (2021).
- 461 28. Bartholomeusz, D. A., Boutte, R. W. & Andrade, J. D. Xurography: rapid prototyping of
462 microstructures using a cutting plotter. *J. Microelectromech. Syst.* **14**, 1364–1374 (2005).
- 463 29. Nath, P. *et al.* Rapid prototyping of robust and versatile microfluidic components using adhesive
464 transfer tapes. *Lab Chip* **10**, 2286–2291 (2010).
- 465 30. Chang, N. *et al.* Low cost 3D microfluidic chips for multiplex protein detection based on photonic
466 crystal beads. *Lab Chip* **18**, 3638–3644 (2018).
- 467 31. Patko, D. *et al.* Microfluidic channels laser-cut in thin double-sided tapes: Cost-effective
468 biocompatible fluidics in minutes from design to final integration with optical biochips. *Sens.*
469 *Actuators B Chem.* **196**, 352–356 (2014).

- 470 32. Kim, J., Surapaneni, R. & Gale, B. K. Rapid prototyping of microfluidic systems using a
471 PDMS/polymer tape composite. *Lab Chip* **9**, 1290–1293 (2009).
- 472 33. Yuen, P. K. & Goral, V. N. Low-cost rapid prototyping of flexible microfluidic devices using a desktop
473 digital craft cutter. *Lab Chip* **10**, 384–387 (2010).
- 474 34. Lai, X. *et al.* Sticker Microfluidics: A Method for Fabrication of Customized Monolithic Microfluidics.
475 *ACS Biomater Sci Eng* **5**, 6801–6810 (2019).
- 476 35. Khashayar, P. *et al.* Rapid prototyping of microfluidic chips using laser-cut double-sided tape for
477 electrochemical biosensors. *J. Brazil. Soc. Mech. Sci. Eng.* **39**, 1469–1477 (2017).
- 478 36. Unger, M. A., Chou, H. P., Thorsen, T., Scherer, A. & Quake, S. R. Monolithic microfabricated valves
479 and pumps by multilayer soft lithography. *Science* **288**, 113–116 (2000).
- 480 37. Cha, J. *et al.* A highly efficient 3D micromixer using soft PDMS bonding. *J. Micromech. Microeng.* **16**,
481 1778 (2006).
- 482 38. Satyanarayana, S., Karnik, R. N. & Majumdar, A. Stamp-and-stick room-temperature bonding
483 technique for microdevices. *J. Microelectromech. Syst.* **14**, 392–399 (2005).
- 484 39. Lee, N. Y. & Chung, B. H. Novel poly(dimethylsiloxane) bonding strategy via room temperature
485 “chemical gluing.” *Langmuir* **25**, 3861–3866 (2009).
- 486 40. Martynova, L. *et al.* Fabrication of plastic microfluid channels by imprinting methods. *Anal. Chem.*
487 **69**, 4783–4789 (1997).
- 488 41. Gendron, P.-O., Avaltroni, F. & Wilkinson, K. J. Diffusion coefficients of several rhodamine
489 derivatives as determined by pulsed field gradient-nuclear magnetic resonance and fluorescence
490 correlation spectroscopy. *J. Fluoresc.* **18**, 1093–1101 (2008).
- 491 42. Oshinowo, O. *et al.* Significant differences in single-platelet biophysics exist across species but
492 attenuate during clot formation. *Blood Adv* **5**, 432–437 (2021).

- 493 43. Myers, D. R. *et al.* Single-platelet nanomechanics measured by high-throughput cytometry. *Nat.*
494 *Mater.* **16**, 230–235 (2017).
- 495 44. van der Walt, S. *et al.* scikit-image: image processing in Python. *PeerJ* **2**, e453 (2014).
- 496 45. Neeves, K. B. & Diamond, S. L. A membrane-based microfluidic device for controlling the flux of
497 platelet agonists into flowing blood. *Lab Chip* **8**, 701–709 (2008).
- 498 46. Colace, T. V., Fogarty, P. F., Panckeri, K. A., Li, R. & Diamond, S. L. Microfluidic assay of hemophilic
499 blood clotting: distinct deficits in platelet and fibrin deposition at low factor levels. *J. Thromb.*
500 *Haemost.* **12**, 147–158 (2014).
- 501 47. Schoeman, R. M., Lehmann, M. & Neeves, K. B. Flow chamber and microfluidic approaches for
502 measuring thrombus formation in genetic bleeding disorders. *Platelets* **28**, 463–471 (2017).
- 503 48. Zhu, S. *et al.* In microfluidico: Recreating in vivo hemodynamics using miniaturized devices.
504 *Biorheology* **52**, 303–318 (2015).
- 505 49. Templin, M. F. *et al.* Protein microarray technology. *Trends Biotechnol.* **20**, 160–166 (2002).
- 506 50. Ghosh, S. & Ahn, C. H. Lyophilization of chemiluminescent substrate reagents for high-sensitive
507 microchannel-based lateral flow assay (MLFA) in point-of-care (POC) diagnostic system. *Analyst*
508 **144**, 2109–2119 (2019).
- 509 51. Sackmann, E. K., Fulton, A. L. & Beebe, D. J. The present and future role of microfluidics in
510 biomedical research. *Nature* **507**, 181–189 (2014).
- 511 52. He, X., Wang, B., Meng, J., Zhang, S. & Wang, S. How to Prevent Bubbles in Microfluidic Channels.
512 *Langmuir* **37**, 2187–2194 (2021).